upward. The intramolecular contacts between the titanyl oxygen atom and the methyl carbon atoms on the saturated meso-carbon atoms $(O\cdots C_1)$ are 3.41 Å.

References and Notes

(1) (a) University of Notre Dame. (b) Technischen Hochschule Aachen.
(2) D. Mauzerall and S. Granick, *J. Biol. Chem.*, **232**, 1141 (1958).
(3) R. B. Woodward, *Angew. Chem.*, **72**, 651 (1960).
(4) A. Treibs and H. Häberle, *Justus Liebigs Ann. Chem.*, **718**, 183 (1968).
(5) D. Dolphin, *J. Heterocycl. Chem.*, 7, 275 (1970).
(6) J. W. Buchler, L. Puppe, and H. H. Schneehage, *Justus Liebigs Ann. Chem.*, **749**, 134 (1971).
(7) J. W. Buchler and H. H. Schneehage, *Tetrahedron Lett.*, 3803 (1972).
(8) G. R. Seely and K. Talmadge, *Photochem. Photobiol.*, 3 195 (1964).
(9) A. N. Sidorov, *Biofizika*, 10, 226 (1965).
(10) H. Scheer and J. J. Katz, *Proc. Natl. Acad. Sci. U.S.A.*, **71**, 1626 (1974).
(11) P. N. Dwyer, J. W. Buchler, and W. R. Scheidt, *J. Am. Chem. Soc.*, **96**, 2789 (1974).

(12) J. W. Buchler and L. Puppe, *Justus Liebigs Ann. Chem.*, 1046 (1974).
(13) A structure determination of octaethylporphinatooxotitanium(IV) is in progress: U. Thewalt and J. H. Fuhrhop, personal communication.
(14) W. R. Scheidt, *J. Am. Chem. Soc.*, **96**, 84 (1974).
(15) The function minimized was $\sum w(|F_o| - k|F_c|)^2$. The computations followed W. R. Busing, K. O. Martin, and H. A. Levy, "OR-FLS, a Fortran Crystallographic Least-Squares Program", Report ORNL-TM-305, Oak Ridge National Laboratory, Oak Ridge, Tenn., 1962. Atomic form factors were from D. T. Cromer and J. B. Mann, *Acta Crystallogr., Sect. A*, **24**, 321 (1968), with corrections, real and imaginary, for the anomalous scattering of the titanium atom from D. T. Cromer and D. Liberman, *J. Chem. Phys.*, **53**, 1891 (1970). The Fourier program ALFF was used: C. R. Hubbard, C. O. Quicksall, and R. A. Jacobson, "The Fast Fourier Algorithm and the Programs ALFF, ALFFDP, ALFFPROJ, ALFFT, and FRIEDEL", Report IS-2625, Ames Laboratory, Iowa State University, Ames, Iowa, 1971.
(16) Supplementary material.
(17) C. K. Johnson, "ORTEP, a Fortran Thermal-Ellipsoid Plot Program for Crystal Structure Illustrations", Report ORNL-3794, Oak Ridge National Laboratory, Oak Ridge, Tenn., 1965.
(18) These calculations followed W. R. Busing, K. O. Martin, and H. A. Levy, "ORFFE, a Fortran Crystallographic Function and Error Program", Report ORNL-TM-306, Oak Ridge National Laboratory, Oak Ridge, Tenn., 1964.
(19) D. Schwarzenbach, *Inorg. Chem.*, **9**, 2391 (1970).
(20) J. D. Matthews, N. Singer, and A. G. Swallow, *J. Chem. Soc. A*, 2545 (1970); B. F. Studd and A. G. Swallow, *J. Chem. Soc. A*, 1961 (1968).
(21) D. C. Bradley, M. B. Hursthouse, and I. F. Randall, *Chem. Commun.*, 672 (1969).
(22) K. Watenpaugh and C. N. Caughlin, *Inorg. Chem.*, **6**, 963 (1967).
(23) R. C. Pettersen, *Acta Crystallogr., Sect. B*, **25**, 2527 (1969); J. G. Forrest and C. K. Prout, *J. Chem. Soc. A*, 1312 (1967); P. K. Hon, R. L. Belford, and C. E. Pfluger, *J. Chem. Phys.*, **43**, 1323 (1965); R. P. Dodge, D. H. Templeton, and A. Zalkin, *ibid.*, **35**, 55 (1961); N. D. Chasteen, R. L. Belford, and I. C. Paul, *Inorg. Chem.*, **8**, 408 (1969); M. Mathew, A. J. Carty, and G. J. Palenik, *J. Am. Chem. Soc.*, **92**, 3197 (1970).
(24) W. R. Scheidt, C.-C. Tsai, and J. L. Hoard, *J. Am. Chem. Soc.*, **93**, 3867 (1971), and succeeding papers; W. R. Scheidt, *Inorg. Chem.*, **12**, 1758 (1973); R. R. Ryan, S. H. Mastin, and M. J. Reisfeld, *Acta Crystallogr., Sect. B*, **27**, 1270 (1971).
(25) W. Haase and H. Hoppe, *Acta Crystallogr., Sect. B*, **24**, 281 (1968).

Contribution from the Department of Chemistry,
Simon Fraser University, Burnaby, British Columbia, Canada V5A 1S6

An Asymmetrically Coordinated Diperoxo Compound. Crystal Structure of $K_3[VO(O_2)_2(C_2O_4)]\cdot H_2O$

D. BEGIN, F. W. B. EINSTEIN,* and J. FIELD

Crystals of $K_3[VO(O_2)_2(C_2O_4)]\cdot H_2O$ are monoclinic with $a = 7.100$ (2) Å, $b = 7.857$ (2) Å, $c = 17.421$ (4) Å, $\beta = 98.45$ (2)°, $Z = 4$, and space group $P2_1/c$. A total of 2205 counter intensities were measured of which 1900 ($>2.3\sigma$) were used to refine the structure by least-squares methods to $R = 5.6\%$. The anion is pentagonal bipyramidal in shape, the vanadyl oxygen atom (1.622 (4) Å) at one apex. Two asymmetrically coordinated (1.861 (4) and 1.923 (4) Å) peroxy groups are related by an approximate anionic mirror plane. The two oxygen atoms involved in the shorter bonds are adjacent (O···O = 2.56 Å). The coordinated oxalate group has V–O distances 2.060 (4) and 2.251 (4) Å (apical). The vanadium atom is 0.28 Å above the approximate pentagonal plane comprising the two peroxo groups and one of the oxalate oxygen atoms. The water molecule is weakly involved in hydrogen bonds to oxalate and peroxo groups.

Introduction

Structural data on mononuclear transition metal–diperoxo compounds include determinations of structure for V(V),[1] Nb(V),[2] Cr(IV),[3-5] Cr(VI),[6-8] and Mo(VI)[9] complexes. The seven-coordinate species[10] have pentagonal-bipyramidal coordination geometries while the two examples of six-coordination, the $CrO(O_2)_2(C_5H_5N)$ molecule[8] and the $[VO(O_2)_2NH_3]^-$ anion,[1] have distorted pentagonal-pyramidal geometries. The eight-coordinate $[Nb(O_2)_2(C_2O_4)_2]^{3-}$ anion[2] has a quasidodecahedral structure similar to that reported for the triperoxoniobate(V) anion $[Nb(O_2)_3(C_{12}H_8N_2)]^-$,[12] the tetraperoxoniobate(V) compound $KMg[Nb(O_2)_4]\cdot7H_2O$,[13] and the tetraperoxochromium(V) compound $K_3[Cr(O_2)_4]$.[14,15] The peroxo groups in the $[Cr(O_2)_4]^{3-}$ anion are asymmetrically π bonded to the chromium ion, i.e., the chromium ion is nearer to one oxygen of the peroxo group than to the other. A ligand

field calculation, based on the optical and electron paramagnetic resonance spectra for this unusual d^1 system, has accounted for the significant difference in Cr–O peroxo bond lengths.[15] To continue the structural study of mononuclear transition metal–diperoxo compounds, the crystal structure of the seven-coordinate $K_3[VO(O_2)_2(C_2O_4)]\cdot H_2O$ compound has been determined.

Experimental Section

Large orange crystals of $K_3[VO(O_2)_2(C_2O_4)]\cdot H_2O$ were prepared using the method reported by Vuletic and Djordjevic.[16] The crystal chosen to collect the complete diffraction data (obtained over a period of ca. 3 weeks) had dimensions 0.40 × 0.12 × 0.06 mm with the a axis along the longest dimension; no decomposition was observed.

On the basis of Weissenberg and precession photographs the crystals were assigned to the monoclinic system. The observed systematic absences are $h0l$ for l odd and $0k0$ for k odd, confirming space group

Table I. Final Positional and Thermal Parameters for $K_3[VO(O_2)_2(C_2O_4)]\cdot H_2O$

Atom	x/a	y/b	z/c	U, Å^2
V	−0.2476 (1)^a	0.2200 (1)	0.3348 (1)	b
K(1)	−0.8532 (2)	0.1779 (2)	0.2034 (1)	b
K(2)	−0.7952 (2)	0.0534 (2)	0.4224 (1)	b
K(3)	−0.3341 (2)	0.0235 (2)	0.1555 (1)	b
O(1)	−0.0092 (5)	0.3296 (6)	0.3238 (2)	b
O(2)	−0.1551 (6)	0.3389 (6)	0.2555 (2)	b
O(3)	−0.4883 (6)	0.2457 (6)	0.2779 (3)	b
O(4)	−0.5017 (6)	0.1858 (6)	0.3557 (3)	b
O(5)	−0.1478 (6)	0.1845 (5)	0.4508 (2)	b
O(6)	−0.2932 (5)	0.4691 (5)	0.3933 (2)	b
O(7)	−0.1033 (6)	0.2904 (6)	0.5701 (2)	b
O(8)	−0.2693 (7)	0.5913 (7)	0.5097 (2)	b
O(9)	−0.1909 (6)	0.0258 (6)	0.3166 (3)	b
O(10)	−0.4791 (6)	0.8415 (8)	0.4205 (4)	b
C(1)	−0.1564 (8)	0.3034 (7)	0.5005 (3)	b
C(2)	−0.2473 (7)	0.4710 (7)	0.4658 (3)	b
H(1)	−0.42 (2)	0.90 (2)	0.393 (6)	0.063^c
H(2)	−0.39 (2)	0.76 (2)	0.445 (5)	0.063^c

Atom	U_{11} ^{b}	U_{22}	U_{33}	U_{12}	U_{13}	U_{23}
V	0.0206 (5)	0.0125 (5)	0.0139 (4)	0.0006 (3)	0.0027 (3)	−0.0027 (4)
K(1)	0.0258 (6)	0.0202 (7)	0.0205 (6)	0.0024 (5)	0.0021 (5)	−0.0050 (5)
K(2)	0.0323 (7)	0.0286 (8)	0.0495 (9)	0.0051 (6)	0.0144 (7)	0.0152 (7)
K(3)	0.0248 (6)	0.0250 (7)	0.0170 (6)	−0.0031 (5)	0.0036 (5)	−0.0007 (5)
O(1)	0.019 (2)	0.034 (3)	0.018 (2)	−0.002 (2)	0.004 (2)	−0.002 (2)
O(2)	0.025 (2)	0.028 (2)	0.017 (2)	−0.001 (2)	0.003 (2)	0.001 (2)
O(3)	0.027 (2)	0.031 (3)	0.021 (2)	−0.000 (2)	−0.001 (2)	−0.003 (2)
O(4)	0.025 (2)	0.033 (3)	0.029 (2)	−0.006 (2)	0.010 (2)	0.001 (2)
O(5)	0.032 (2)	0.014 (2)	0.016 (2)	0.007 (2)	0.003 (2)	0.002 (2)
O(6)	0.025 (2)	0.019 (2)	0.007 (2)	0.002 (2)	0.001 (2)	0.003 (2)
O(7)	0.034 (2)	0.027 (3)	0.015 (2)	−0.001 (2)	0.001 (2)	0.001 (2)
O(8)	0.050 (3)	0.018 (2)	0.016 (2)	0.008 (2)	0.004 (2)	−0.001 (2)
O(9)	0.039 (3)	0.019 (2)	0.026 (2)	0.009 (2)	0.003 (2)	−0.004 (2)
O(10)	0.048 (4)	0.034 (3)	0.094 (6)	0.012 (3)	0.022 (3)	0.029 (3)

^{a} Estimated standard errors of the least significant figures are given in parentheses here and in subsequent tables. ^{b} Anisotropic thermal parameters. The form of the anisotropic thermal ellipsoid is $\exp[-2\pi^2(h^2a^{*2}U_{11} + \ldots + 2hka^*b^*U_{12} + \ldots)]$. ^{c} Fixed isotropic temperature factors.

$P2_1/c$. Precise cell parameters were determined by the least-squares refinement of the 2θ values ($2\theta > 48°$), for 12 reflections which had been accurately centered on the Mo Kα_1 peak (λ 0.70926 Å), using an automatic Picker four-circle diffractometer. The takeoff angle was 1.0° and the temperature was 22°. The cell parameters are $a = 7.100$ (2) Å, $b = 7.857$ (2) Å, $c = 17.421$ (4) Å, and $\beta = 98.45$ (2)°. The density calculated for four formula weights per unit cell is 2.448 g cm^{-3} and compares with that of 2.45 (2) g cm^{-3} measured by flotation in a CH$_3$I–CH$_2$I$_2$ mixed-solvent system.

The crystal was mounted on the diffractometer with the a axis slightly offset from the spindle axis. Intensity data were collected by the θ–2θ scan technique using monochromatized Mo Kα radiation (graphite monochromator) and a scintillation counter equipped with pulse height analysis. The scan rate was 2.0° min^{-1}, and the scan range was ±0.6° in 2θ from a position calculated using the intensity-weighted average of the Kα_1 and Kα_2 peaks (λ 0.71069 Å). During data collection the takeoff angle was 3.0° and the detector, with an aperture 5.0 mm high and 4.0 mm wide, was positioned 28 cm from the crystal. The background intensity was determined by the normalization of two stationary-background counts of 10 sec measured at both scan limits. Two standard reflections were measured every 70 reflections and retained a constancy of within 2% over the entire data collection.

A unique data set having $2\theta < 55°$ was obtained. The values of I and $\sigma(I)$[17] were corrected for Lorentz and polarization[18] effects; a value of 0.03 was used for the precision constant. No absorption corrections were made ($\mu = 22.6$ cm^{-1}); the extreme error that this would introduce is ±5.0% in I. Of the 2205 unique reflections measured, 1900 have intensities greater than $2.3\sigma(I)$; only these were used in the solution and refinement of the structure.

Structure Determination and Refinement

The symbolic addition procedure[19,20] was used to initiate the solution of the structure in space group $P2_1/c$. E values were determined, and the origin was fixed by arbitrarily assigning phases to three of the stronger E's (3, 2, −20, $E = +3.24$; 6, −5, 8, $E = +2.84$; 2, 3, −15, $E = +2.57$). The first F_o Fourier synthesis, using those

signed reflections with $E \geq 2.0$, revealed the positions of the vanadium and potassium atoms. A F_o fourier map, phased on the refined heavy-atom coordinates, gave the positions of all the remaining nonhydrogen atoms.

Refinement of the structure was carried out by full-matrix least-squares techniques; the function minimized was $\sum w(|F_o| - |F_c|)^2$ and each reflection was given weight $[=1/\sigma^2(F)]$ in terms of $\sigma(F) = \sigma(I)/(Lp)(2F_o)$. Initial isotropic refinement and subsequent difference Fourier syntheses indicated anisotropic thermal motion by all the nonhydrogen atoms; several cycles of anisotropic refinement reduced R[21] to 0.056 and R_w[21] to 0.081. A difference Fourier synthesis gave the positions of both hydrogen atoms; during further refinement their positions were allowed to vary but their isotropic temperature factors were fixed at a constant value of $B = 5.0$ Å^2. In the final cycle of least-squares refinement ($R = 0.056$, $R_w = 0.078$), no parameter underwent a shift in excess of 6% of its estimated standard deviation.

A final difference Fourier synthesis showed no unusual features; the largest peak was close to the vanadium atom with peak height 0.5 (3) e Å^{-3}. Neutral atomic scattering factors for the nonhydrogen atoms were taken from ref 22 and included corrections for anomalous dispersion to the vanadium and potassium atoms.[23] Hydrogen atomic scattering factors were taken from ref 24. Crystallographic programs used in this determination have been cited elsewhere.[25]

A table of measured and calculated structure factors is available.[26] The positional and thermal parameters derived from the final least-squares cycle are given in Table I.

Discussion

Crystals of $K_3[VO(O_2)_2(C_2O_4)]\cdot H_2O$ contain four formula units in the primitive monoclinic unit cell with the potassium ions, oxodiperoxooxalatovanadate(V) anions, and water molecules held together by electrostatic forces and hydrogen bonding. Bond lengths and angles are given in Table IIa and b, respectively. The vanadium atom is seven-coordinate and has a pentagonal-bipyramidal environment; the two peroxo
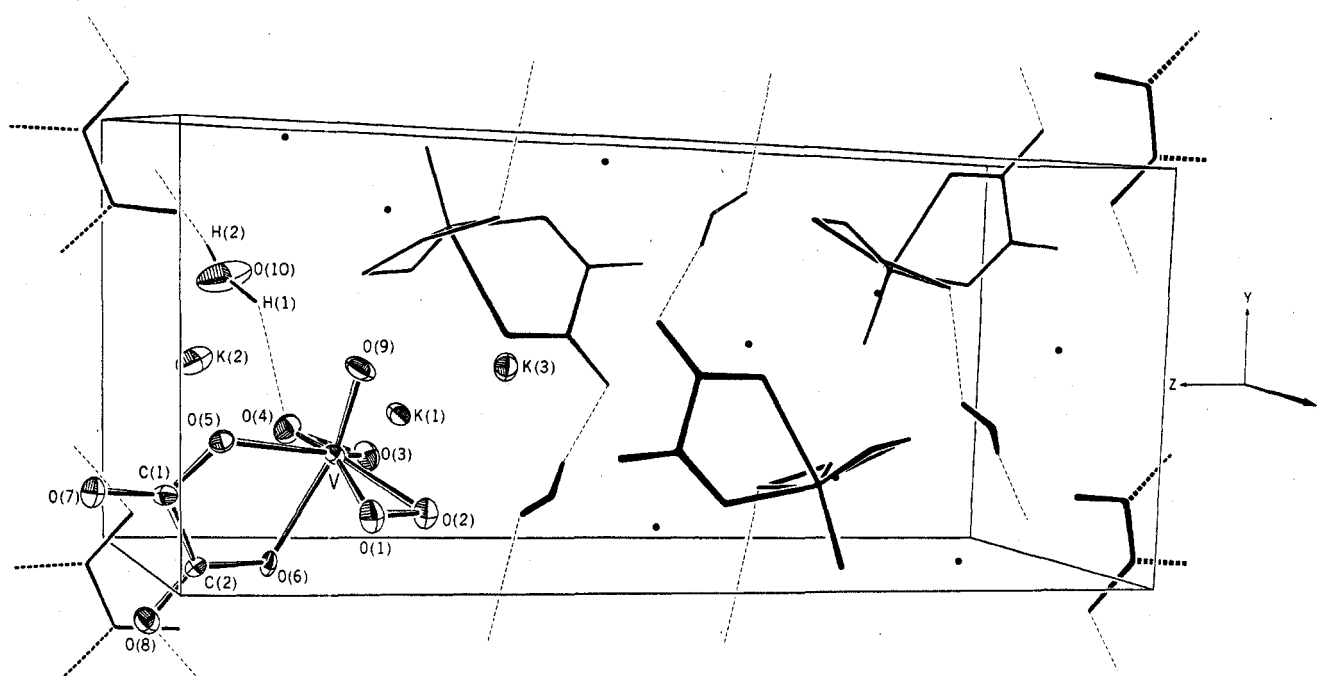
Figure 1. The unit cell of $K_3[VO(O_2)_2(C_2O_4)]\cdot H_2O$ showing the atomic labeling. Nonhydrogen atoms in the asymmetric unit are shown as 50% probability thermal ellipsoids. Broken lines indicate hydrogen bonds.

groups and one oxygen atom from the oxalate ligand make up the pentagonal girdle, while the oxo ligand and an oxygen atom of the oxalato group occupy the apical positions (see Figure 1). The least-squares plane through the oxalate ligand atoms, the vanadium, and the vanadyl oxygen atoms defines an approximate mirror plane for the anion (plane 1; see Table III). Thus the $[VO(O_2)_2(C_2O_4)]^{3-}$ anion has approximate C_s-m symmetry, in common with other mononuclear, six- and seven-coordinate transition metal–diperoxo species (see Table IV).

The vanadium atom is displaced 0.28 Å from the pentagonal plane (plane 2) toward the double-bonded oxygen, O(9). This arrangement is characteristic of oxovanadium(V),[1,25,27,28] oxochromium(VI),[6–8] and oxomolybdenum(VI)[9,29] compounds and is attributed[30] to repulsions between the metal–oxygen π bonds in the equatorial plane. Stomberg[5] has divided mononuclear diperoxo species into two types: those which include a double-bonded oxo ligand (type II) and those which do not (type I). The type I diperoxo species listed in Table IV have the central metal atom and the five atoms comprising the pentagonal girdle, coplanar within experimental error. In contrast the displacement (d) of the metal atom from the pentagonal plane is highly significant for both the pentagonal-pyramidal and pentagonal-bipyramidal species of type II. For the seven-coordinate species values of d fall in the range 0.27–0.35 Å while the six-coordinate species have d values which are somewhat greater (0.46 Å in the [V-O(O_2)_2NH_3]$^-$ anion[1] and 0.51 Å in the [CrO(O_2)_2py] molecule[8]).

The V–O$_{peroxo}$ bond lengths in the $[VO(O_2)_2(C_2O_4)]^{3-}$ anion divide into two distinct pairs. Those which are cis to the V–O(5) bond (V–O$_{cis}$) are significantly greater than the V–O$_{peroxo}$ bonds which make an angle of approximately 135° with the V–O(5) bond (V–O$_{trans}$). This notation is illustrated in Figure 2. In fact the values observed (1.856–1.934 Å) span the range of V–O$_{peroxo}$ distances previously reported: 1.872 (2) Å in the [VO(O_2)(H_2O)(C_5H_3N(COO)_2)]$^-$ anion,[25] 1.85–1.87 Å in the dinuclear [O(VO(O_2)_2]$^-$ anion,[27] and 1.883 (3) Å in the [VO(O_2)_2NH_3]$^-$ anion.[1] Differences between the V–O$_{cis}$ and V–O$_{trans}$ bond lengths for the individual peroxo groups are 0.068 (6) and 0.055 (6) Å. Clearly these differences
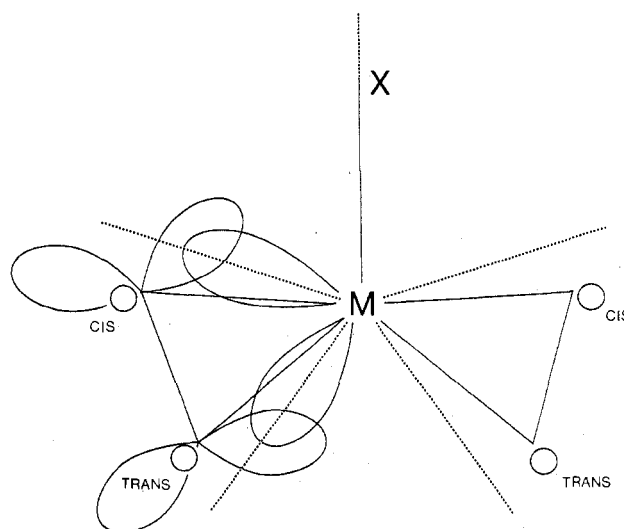

Figure 2. Pentagonal plane for mononuclear six- and seven-coordinate transition metal–diperoxo compounds (M = transition metal; X = C, N, or O atom).

are significant, whereas current bonding models[31,32] for the peroxo group coordinated to a transition metal in a d^0-configuration do not predict unequal metal–O$_{peroxo}$ bond lengths; i.e., the filled antibonding π orbitals on the O_2^{2-} ion would be expected to overlap to the same extent with orbitals of appropriate symmetry on the central metal atom (see Figure 2); hence we have the formation of metal–O$_{peroxo}$ σ bonds which are "bent" with respect to the internuclear axis.[33] (It should be noted that the molecular orbital scheme we have used for the O_2^{2-} ion is very similar to that for ethylene; i.e., the oxygen atoms are sp^2 hybridized with the four lone pairs replacing the C–H bonds.[32])

Mingos[32] has suggested that severe nonbonded repulsions involving the peroxo group oxygen atoms may influence the transition metal–peroxo group geometry. Clearly, for the pentagonal-pyramidal and pentagonal-bipyramidal species listed in Table IV, nonbonded repulsions between atoms in the pentagonal girdle are critical in determining any "in-plane"

Table II. Interatomic Distances (Å) and Angles (deg)[a]

(a) Bond Distances

V–O(1)	1.934 (4)	O(1)–O(2)	1.460 (6)
V–O(2)	1.866 (4)	O(3)–O(4)	1.451 (6)
V–O(3)	1.856 (4)	O(5)–C(1)	1.282 (7)
V–O(4)	1.911 (4)	O(6)–C(2)	1.258 (7)
V–O(5)	2.060 (4)	O(7)–C(1)	1.219 (7)
V–O(6)	2.251 (4)	O(8)–C(2)	1.241 (7)
V–O(9)	1.622 (4)	C(1)–C(2)	1.550 (8)
		H(1)–O(10)	0.78 (10)
		H(2)–O(10)	0.93 (10)

(b) Bond Angles

O(1)–V–O(2)	45.2 (2)	V–O(1)–O(2)	65.0 (2)
O(1)–V–O(3)	130.5 (2)	V–O(2)–O(1)	70.0 (2)
O(1)–V–O(4)	161.1 (2)	V–O(3)–O(4)	69.4 (2)
O(1)–V–O(5)	88.8 (2)	V–O(4)–O(3)	65.4 (2)
O(1)–V–O(6)	81.0 (2)	V–O(5)–C(1)	121.3 (4)
O(1)–V–O(9)	98.8 (2)	V–O(6)–C(2)	115.5 (4)
O(2)–V–O(3)	87.0 (2)		
O(2)–V–O(4)	131.1 (2)	O(5)–C(1)–O(7)	124.9 (5)
O(2)–V–O(5)	133.4 (2)	O(5)–C(1)–C(2)	114.5 (5)
O(2)–V–O(6)	89.4 (2)	O(7)–C(1)–C(2)	120.6 (5)
O(2)–V–O(9)	101.6 (2)	O(6)–C(2)–O(8)	126.2 (5)
O(3)–V–O(4)	45.3 (2)	O(6)–C(2)–C(1)	114.5 (5)
O(3)–V–O(5)	134.1 (2)	O(8)–C(2)–C(1)	119.3 (5)
O(3)–V–O(6)	88.0 (2)	H(1)–O(10)–H(2)	106 (9)
O(3)–V–O(9)	103.5 (2)		
O(4)–V–O(5)	89.6 (2)		
O(4)–V–O(6)	80.4 (2)		
O(4)–V–O(9)	100.0 (2)		
O(5)–V–O(6)	74.1 (2)		
O(5)–V–O(9)	90.3 (2)		
O(6)–V–O(9)	164.4 (2)		

(c) Hydrogen Bond Parameters[b]

O(10)···O(4)[I]	2.927 (8)	O(10)–H(1)···O(4)[I]	123 (9)
H(1)···O(4)[I]	2.4 (1)		
O(10)···O(8)	2.796 (8)	O(10)–H(1)···O(8)	165 (9)
H(2)···O(8)	1.9 (1)		
O(10)···O(9)[I]	3.263 (7)	O(10)–H(1)···O(9)[I]	169 (10)
H(1)···O(9)[I]	2.5 (1)		

(d) Potassium–Oxygen Distances Less Than 3.2 Å[b]

K(1)···O(1)[II]	2.781 (4)	K(2)···O(8)[VII]	3.040 (5)
K(1)···O(1)[III]	2.921 (5)	K(2)···O(9)[II]	3.133 (5)
K(1)···O(2)[II]	2.755 (4)	K(2)···O(10)[VIII]	2.799 (6)
K(1)···O(2)[III]	2.757 (5)	K(3)···O(1)[IX]	2.852 (4)
K(1)···O(3)	2.774 (4)	K(3)···O(2)	3.184 (4)
K(1)···O(6)[III]	2.668 (4)	K(3)···O(3)[III]	2.852 (5)
K(1)···O(7)[IV]	2.720 (4)	K(3)···O(3)	3.079 (5)
K(1)···O(9)[V]	2.779 (5)	K(3)···O(4)[III]	2.894 (5)
K(2)···O(1)[II]	3.034 (5)	K(3)···O(6)[III]	2.692 (4)
K(2)···O(4)	2.737 (4)	K(3)···O(7)[X]	2.785 (4)
K(2)···O(5)[II]	2.817 (4)	K(3)···O(8)[X]	2.796 (4)
K(2)···O(5)[VI]	2.965 (4)	K(3)···O(9)	2.841 (5)
K(2)···O(7)[VI]	2.804 (5)	K(3)···O(10)[IX]	3.040 (7)

[a] Errors in interatomic distances and angles were calculated from the inverse matrix and include correlation between atomic parameters and errors in the cell dimensions. [b] Superscripts indicate the symmetry operation to be applied: (I) x, $1 + y$, z; (II) $-1 + x$, y, z; (III) $-1 - x$, $-\frac{1}{2} + y$, $\frac{1}{2} - z$; (IV) $-1 + x$, $\frac{1}{2} - y$, $-\frac{1}{2} + z$; (V) $-1 - x$, $\frac{1}{2} + y$, $\frac{1}{2} - z$; (VI) $-1 - x$, $-y$, $1 - z$; (VII) $-1 - x$, $1 - y$, $1 - z$; (VIII) x, $-1 + y$, z; (IX) $-x$, $-\frac{1}{2} + y$, $\frac{1}{2} - z$; (X) x, $\frac{1}{2} - y$, $-\frac{1}{2} + z$.

distortion of the metal–peroxo group geometry. Accordingly we have listed the M–O$_{cis}$, M–O$_{trans}$, O$_{cis}$···X, and O$_{trans}$···O$_{trans}$ distances for mononuclear, six- and seven-coordinate transition metal–diperoxo compounds (M = transition metal; X = C, N, or O atom in the pentagonal plane; see Figure 2). Also shown in Table IV are the mean M–O$_{peroxo}$ bond lengths which give an indication of the size of the central metal ion. We first note that for the majority of the diperoxo species listed in Table IV, the individual peroxo groups have M–O$_{cis}$ and M–O$_{trans}$ distances which agree within three estimated standard de-

viations; however in the case of the [CrO(O$_2$)$_2$bipy],[6] [CrO(O$_2$)$_2$(o-phen)],[7] and [VO(O$_2$)$_2$(C$_2$O$_4$)]$^{3-}$ species the M–O$_{cis}$ bond lengths are significantly greater than the M–O$_{trans}$ bond lengths. The latter three compounds are characterized by a seven-coordinate central metal ion with a relatively small ionic radius;[34] in addition the displacement of the central metal atom from the pentagonal plane toward the oxo ligand has the effect of drawing the atoms in the girdle closer together and increasing nonbonded repulsions between them. In particular the O$_{trans}$···O$_{trans}$ nonbonded contacts for the seven-coordinate chromium(VI) and vanadium(V) species approach the limiting O···O nonbonded distance of 2.50 Å,[35] observed for the seven-coordinate ethylenediaminetetraacetatoaquoferrate(III) ion.[36] The O$_{cis}$···X contacts are substantially longer, the implication being that the O$_{cis}$···X and O$_{trans}$···O$_{trans}$ nonbonded interactions are different. Perhaps this is not surprising as the X atoms are distinguished by π systems which protrude in the pentagonal plane. Certainly, nonbonded repulsions of the type O$_{cis}$···X are minimized by a lengthening of the M–O$_{cis}$ bond relative to the M–O$_{trans}$ bond (see Figure 2).

Nonbonded repulsions between atoms comprising the pentagonal girdle may also be reduced by marked deviations of the five atoms from coplanarity (deviations >0.10 Å from the least-squares mean plane). This occurs for the six-coordinate pentagonal-pyramidal species; in both the [CrO-(O$_2$)$_2$py] molecule[8] and the [VO(O$_2$)$_2$NH$_3$]$^-$ anion,[1] the X atom and the O$_{cis}$ peroxo oxygen atoms lie on opposite sides of the least-squares plane. As may be expected, the seven-coordinate pentagonal-bipyramidal species exhibit well-defined pentagonal planes (deviations <0.05 Å from the least-squares mean plane). Presumably the two apical ligands provide nonbonded contacts which promote this situation. Finally, it should be noted that asymmetric coordination of the peroxo group could possibly be the product of attractive rather than repulsive forces. In particular the short M–O$_{trans}$ and O$_{trans}$···O$_{trans}$ distances may derive from overlap of the M–O$_{trans}$ "bent" σ bonds; this would lead to a three-center bonding situation, involving σ-orbital contributions from the two O$_{trans}$ peroxo oxygen atoms and the transition metal atom (see Figure 2).

The V=O bond length in the [VO(O$_2$)$_2$(C$_2$O$_4$)]$^{3-}$ anion is significantly greater than the value found for the six-coordinate [VO(O$_2$)$_2$NH$_3$]$^-$ anion [1.606 (3) Å],[1] since not only is there an additional ligand atom but also it is competitively positioned with respect to the oxo ligand. Other V=O bond lengths reported for vanadium–peroxo compounds are 1.579 (2) Å in the [VO(O$_2$)(H$_2$O)(C$_5$H$_3$N(COO)$_2$)]$^-$ anion[25] and 1.58 (2) and 1.64 (2) Å in the (NH$_4$)$_4$[O(VO(O$_2$)$_2$)$_2$] compound.[27] The latter two values are relatively inaccurate and are not strictly comparable, while the surprisingly short V=O distance reported for the monoperoxo species has been fully discussed in ref 25. Comparison of the C–O$_{oxalate}$ bond lengths shows that they are significantly different [0.191 (6) Å], the V–O(6) bond being weakened since it is trans to an oxo ligand which has a well-established structural trans effect.[37] Presumably, the V–O(5) distance is regarded as a typical value for a σ bond;[38] similar values of 2.053 (2) and 1.064 (2) Å have been reported for the V–O σ bonds in the seven-coordinate [VO(O$_2$)(H$_2$O)(C$_5$H$_3$N(COO)$_2$)]$^-$ anion.[25]

The peroxo bond lengths show an insignificant difference and fall within the range of O–O distances previously reported for a peroxo group coordinated to a transition metal [1.36–1.54 Å].[39] Other workers[25,31] have noted a correlation between M–O$_{peroxo}$ bond strength and O–O bond order, which has been attributed[15,25,31] to withdrawal of electron density from the antibonding π^* orbitals on the peroxo group to empty orbitals on the central metal atom; i.e., the more strongly the peroxo

Table III. Weighted[a] Least-Squares Mean Planes of the Form $AX + BY + CZ + D = 0$[b]

Plane no.	Atoms	A	B	C	D	X^2
1	V, O(5), O(6), O(7), O(8), O(9), C(1), C(2)	0.9369	0.3203	−0.1401	2.7042	308.3
2	O(1), O(2), O(3), O(4), O(5)	0.2408	−0.9221	−0.3030	4.2475	293.9

Distances of Atoms from Planes, Å

1: V, −0.001; O(1), 1.914; O(2), 1.296; O(3), −1.263; O(4), −1.877; O(5), 0.015;
O(6), 0.042; O(7), 0.004; O(8), −0.053; O(9), −0.025; C(1), 0.018; C(2), 0.002
2: V, 0.276; O(1), −0.046; O(2), 0.036; O(3), 0.011; O(4), −0.033; O(5), 0.027

[a] Atoms are weighted by the reciprocals of their standard deviations. [b] Coordinates (in angstroms) are referred to a right-handed orthogonal system with x and y directed along a and b, respectively.

Table IV. Selected Structural Data (Å) for Mononuclear Six- and Seven-Coordinate Transition Metal–Diperoxo Compounds[a]

Complex	$M-O_{cis}$[b]	$M-O_{trans}$[b]	Mean $M-O_{peroxo}$	Mean O–O	$O_{cis} \cdots X$[b]	$O_{trans} \cdots O_{trans}$[b]	Ref
Type I							
$[M(O_2)_2X_3]$							c
$[Cr(O_2)_2(NH_3)_3]$ I	1.89 (2)	1.88 (2)	1.88 (1)	1.42 (3)	2.88	2.72	d, e
	1.86 (2)	1.87 (2)			2.78		
II	1.91 (2)	1.87 (2)	1.89 (2)	1.45 (3)	2.85	2.70	
$[Cr(O_2)_2(CN)_3]^{3-}$	1.90 (1)	1.87 (1)	1.89 (1)	1.45 (2)	2.71	2.76	f
	1.90 (1)	1.88 (1)			2.80		
$[Cr(O_2)_2(H_2O)en]$	1.91 (2)	1.86 (1)	1.89 (2)	1.46 (2)	2.77	2.69	g, h
Type II							
$[MO(O_2)_2X]$							c
$[CrO(O_2)_2bipy]$	1.92 (1)	1.78 (1)	1.85[i]	1.40 (2)	2.81	2.52	g, j
$[CrO(O_2)_2(o\text{-phen})]$	1.87 (1)	1.80 (1)	1.84[i]	1.40 (2)	2.76	2.55	g, k
$[VO(O_2)_2ox]^{3-}$	1.934 (4)	1.866 (4)	1.89[i]	1.456 (6)	2.79	2.56	l
	1.911 (4)	1.856 (4)			2.80		
$[MoO(O_2)_2ox]^{2-}$	1.95 (2)	1.93 (2)	1.95 (1)	1.46 (3)	2.80	2.66	m
	1.96 (2)	1.94 (2)			2.86		
$[CrO(O_2)_2py]$	1.79 (2)	1.83 (2)	1.82 (1)	1.41 (2)	2.60	2.55	n
	1.80 (2)	1.84 (2)			2.65		
$[VO(O_2)_2NH_3]^-$	1.883 (3)	1.882 (3)	1.883 (3)	1.472 (4)	2.65	2.62	g, o

[a] Abbreviations: en, ethylenediamine; bipy, 2,2′-bipyridyl; o-phen, 1,10-phenanthroline; ox, oxalato; py, pyridine. [b] Notation illustrated in Figure 2. [c] We follow Stomberg's[5] classification of six- and seven-coordinate diperoxo species into type 1 and type II compounds. For type I compounds X = monodentate ligand; for type II compounds X = monodentate or bidentate ligand; M = transition metal. [d] Two independent molecules in the unit cell: molecule I is in a general position while molecule II is situated on a crystallographic mirror plane. [e] Reference 3. [f] Reference 4. [g] Species has crystallographic C_s-m symmetry. [h] Reference 5. [i] Averaging the $M-O_{cis}$ and $M-O_{trans}$ distances is not strictly valid since they show significant differences. [j] Reference 6. [k] Reference 7. [l] This work. [m] Reference 9. [n] Reference 8. [o] Reference 1.

group is coordinated to the metal atom, the shorter the O–O bond length. Mean $M-O_{peroxo}$ and O–O bond lengths for mononuclear, six- and seven-coordinate transition metal–diperoxo compounds are listed in Table IV. They follow the expected trend but the correlation between a strong $M-O_{peroxo}$ bond and a short O–O bond length is not conclusive since changes in bond length are small and standard deviations often large (>0.01 Å).

The C–O bond lengths within the oxalato group fall into two groups depending on which carbon atom they share: type A share C(1) while type B share C(2). Those of type A are significantly different [0.063 (9) Å], as might be expected since the inner C–O bond is adjacent to the stronger V–$O_{oxalate}$ bond.[38] In contrast the C–O bond lengths of type B show an insignificant difference, though it is noteworthy that for both type A and type B the inner C–O bond is weaker. The C–C distance is in good agreement with the sum of the single-bond covalent radii for carbon;[34] a small distortion of the oxalato group from planarity can be described in terms of the angle of twist [2.8 (6)°] of the planar "CO₂" fragments about the C–C bond. Distances and angles observed for the oxalate ligand in the present structure are in good agreement with results of earlier precise determinations of structure for oxalato complexes.[9,38,40]

The water molecule is weakly hydrogen bonded to a peroxo

oxygen atom [O(4)] and to a terminal oxygen atom in the oxalate ligand [O(8)]. Hydrogen-bond parameters are given in Table IIc. It is also noteworthy that H(1) is roughly equidistant from O(4) and O(9), the implication being that the hydrogen bond is bifurcated.[4] Nevertheless the more reliable O(10)···O(9) distance of 3.263 (7) Å is considerably longer than the sum of the van der Waals radii for two oxygen atoms,[34] and we prefer the alternative description of a single hydrogen bond from H(1) to O(4).

The potassium ions have highly irregular oxygen atom environments; potassium–oxygen interatomic distances less than 3.2 Å are listed in Table IId. Remaining intermolecular nonbonded contacts in the crystal structure are all greater than the sum of the van der Waals radii for the two atoms involved.[34]

Supplementary Material Available. A listing of structure factor amplitudes will appear following these pages in the microfilm edition of this volume of the journal. Photocopies of the supplementary

material from this paper only or microfiche (105 × 148 mm, 24× reduction, negatives) containing all of the supplementary material for the papers in this issue may be obtained from the Journals Department, American Chemical Society, 1155 16th St., N.W., Washington, D.C. 20036. Remit check or money order for $4.50 for photocopy or $2.50 for microfiche, referring to code number AIC50153P.

References and Notes

(1) R. E. Drew and F. W. B. Einstein, *Inorg. Chem.*, **11**, 1079 (1972).
(2) G. Mathern and R. Weiss, *Acta Crystallogr., Sect. B.*, **27**, 1572 (1971).
(3) R. Stomberg, *Ark. Kemi.*, **22**, 49 (1964).
(4) R. Stomberg, *Ark. Kemi.*, **23**, 401 (1965).
(5) R. Stomberg, *Ark. Kemi.*, **24**, 47 (1965).
(6) R. Stomberg and I.-B. Ainalem, *Acta Chem. Scand.*, **22**, 1439 (1968).
(7) R. Stomberg, *Ark. Kemi.*, **24**, 111 (1965).
(8) R. Stomberg, *Ark. Kemi.*, **22**, 29 (1964).
(9) R. Stomberg, *Acta Chem. Scand.*, **24**, 2024 (1970).
(10) We prefer to regard the peroxo group as a bidentate ligand, though we recognize that an alternative description of the peroxo group as a π-bonded monodentate ligand is possible.[11]
(11) D. G. Tuck and R. M. Walters, *Inorg. Chem.*, **2**, 428 (1963).
(12) G. Mathern and R. Weiss, *Acta Crystallogr., Sect. B*, **27**, 1572 (1971).
(13) G. Mathern and R. Weiss, *Acta Crystallogr., Sect. B*, **27**, 1598 (1971).
(14) R. Stomberg, *Acta Chem. Scand.*, **17**, 1563 (1963).
(15) J. D. Swalen and J. A. Ibers, *J. Chem. Phys.*, **37**, 17 (1962).
(16) N. Vuletic and C. Djordjevic, *J. Chem. Soc., Dalton Trans.*, 1137 (1973).
(17) A. R. Davis and F. W. B. Einstein, *Inorg. Chem.*, **13**, 1880 (1974).
(18) S. A. Goldfield and K. N. Raymond, *Inorg. Chem.*, **10**, 2604 (1971).
(19) J. Karle and I. L. Karle, *Acta Crystallogr.*, **21**, 849 (1966).
(20) D. Sayre, *Acta Crystallogr.*, **5**, 60 (1952).

(21) *R* is defined as $\sum(|F_o| - |F_c|)/\sum|F_o|$. R_w is defined as $[\sum w(|F_o| - |F_c|)^2/\sum wF_o^2]^{1/2}$.
(22) D. T. Cromer and J. T. Waber, *Acta Crystallogr.*, **18**, 104 (1965).
(23) "International Tables of X-Ray Crystallography", Vol. III, Kynoch Press, Birmingham, England, 1965, Section 3.3.
(24) R. F. Stewart, E. R. Davidson, and W. T. Simpson, *J. Chem. Phys.*, **42**, 3175 (1965).
(25) R. E. Drew and F. W. B. Einstein, *Inorg. Chem.*, **12**, 829 (1973).
(26) Supplementary material.
(27) I.-B. Svensson and R. Stomberg, *Acta Chem. Scand.*, **25**, 898 (1971).
(28) F. W. B. Einstein, E. Enwall, D. M. Morris, and D. Sutton, *Inorg. Chem.*, **10**, 678 (1971).
(29) (a) R. Stomberg, *Acta Chem. Scand.*, **22**, 1076 (1968); (b) I. Larking and R. Stomberg, *ibid.*, **24**, 2043 (1970).
(30) R. J. Gillespie and R. S. Nyholm, *Q. Rev., Chem. Soc.*, **11**, 339 (1957).
(31) R. Stomberg, *Ark. Kemi.*, **24**, 283 (1965), and references therein.
(32) D. M. P. Mingos, *Nature (London)*, **230**, 154 (1971).
(33) W. P. Griffith, *J. Chem. Soc.*, 5248 (1964).
(34) L. Pauling, "The Nature of the Chemical Bond", 3rd ed, Cornell University Press, Ithaca, N.Y., 1960.
(35) J. L. Hoard, *Struct. Chem. Mol. Biol.*, 573, 582 (1968).
(36) M. D. Lind, M. J. Hamor, T. A. Hamor, and J. L. Hoard, *Inorg. Chem.*, **3**, 34 (1964).
(37) T. G. Appleton, H. C. Clark, and L. E. Manzer, *Coord. Chem. Rev.*, **10**, 335 (1973).
(38) W. R. Scheidt, C. C. Tsai, and J. L. Hoard, *J. Am. Chem. Soc.*, **93**, 3867 (1971).
(39) See ref 9 and references therein.
(40) (a) R. E. Drew, F. W. B. Einstein, and S. E. Gransden, *Can. J. Chem.*, **52**, 2184 (1974); (b) G. L. Glen, J. V. Silverton, and J. L. Hoard, *Inorg. Chem.*, **2**, 250 (1963).
(41) W. C. Hamilton and J. A. Ibers, "The Hydrogen Bond", W. A. Benjamin, New York, N.Y., 1968.

Reactions of the Tripod Ligand Tris(2-diphenylphosphinoethyl)phosphine with Cobalt(II) and Nickel(II) Salts and Sodium Borohydride. Structural Characterization of a Five-Coordinate Cobalt(I) Hydride Complex

C. A. GHILARDI, S. MIDOLLINI, and L. SACCONI*
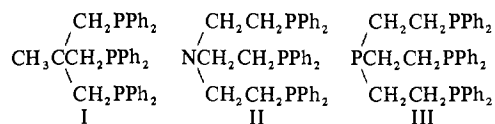
The potentially tetradentate tripod ligand tris(2-diphenylphosphinoethyl)phosphine, pp3, reacts with cobalt(II) salts in the presence of sodium borohydride to give low-spin five-coordinate cobalt(I) complexes [CoX(pp3)], where X = halide, thiocyanate, and hydride. With nickel(II) salts five-coordinate hydrido complexes of the general formula [NiH(pp3)]Y (Y = iodide, tetrafluoroborate, tetraphenylborate) are formed. The cobalt–hydrido complex [CoH(pp3)]·$^1/_2$(CH3)2CO has been characterized by an X-ray structure analysis (trigonal with hexagonal dimensions a = 13.573 (3) Å, c = 36.404 (8) Å, Z = 6, space group $R\bar{3}$) and has been found to have a trigonal-bipyramidal geometry with C_{3v} symmetry. On the basis mainly of the electronic spectra the same geometry must be attributed to all of the cobalt(I) complexes.

Introduction

In recent years many reactions of 3d transition metal ions with tertiary phosphines and a reducing agent such as borohydride have been reported.[1-11] Most reactions involved mono- or bidentate phosphines.[1-3,9] In this laboratory we have investigated the reactions of ligands with three phosphorus atoms in order to examine the effect of increasing denticity. The two ligands used so far have a "tripod" structure. 1,-1,1-Tris(diphenylphosphinomethyl)ethane, p3, I, reacts with cobalt(II) and nickel(II) halides to give, in the presence of borohydride, tetrahedral complexes of the monovalent metal ions with the formula [MX(p3)].[4,12] Tris(2-diphenylphosphinoethyl)amine, np3, II, reacts in an analogous way to give the trigonal-bipyramidal complexes [MX(np3)].[10] When an anion is used which does not coordinate strongly to the metal ion, complexes of the zerovalent metal, such as [Ni(np3)], are obtained.[6,10] This complex is the first one known to have a trigonal-pyramidal structure. Alternatively, the first coordination sphere may become filled by a hydride ion as in the

nonstoichiometric compounds [NiH$_x$(np3)]Y (Y = BF4, ClO4, NO3)[8] or the triply bridged dimer [(p3)CoH3Co(p3)BPh4.[11] Iron(II) forms an analogous dimer.[5,11]

$$
\begin{array}{ccc}
\underset{\diagdown}{\overset{\diagup}{CH_3CCH_2PPh_2}} & \underset{\diagdown}{\overset{\diagup}{NCH_2CH_2PPh_2}} & \underset{\diagdown}{\overset{\diagup}{PCH_2CH_2PPh_2}} \\
CH_2PPh_2 & CH_2CH_2PPh_2 & CH_2CH_2PPh_2 \\
\text{I} & \text{II} & \text{III}
\end{array}
$$

In this work we describe the reactions of the tetraphosphine tris(2-diphenylphosphinoethyl)phosphine, pp3, III, which is similar to the ligand np3 but has a phosphorus atom in the apical position instead of a nitrogen atom. We have prepared and characterized 11 compounds of cobalt and nickel and have determined the X-ray structure of one of them, [CoH-(pp3)]·$^1/_2$(CH3)2CO.

Some metal complexes of this ligand have been recently described;[7,13-15] as far as the 3d transition metals are concerned, pentacoordinate complexes of iron(II), cobalt(II), and nickel(II) have been reported,[13] along with carbonyl derivatives